Electronic Density Fluctuations in Disordered Systems. 1. Effect of Thermal Treatments on the Dynamics and Local Microstructure of Poly(methyl methacrylate)

A. Faivre, L. David,* R. Vassoille, and G. Vigier

Groupe d'Etudes de Métallurgie Physique et de Physique des Matériaux, UMR CNRS 5510, Institut National des Sciences Appliquées de Lyon, Bât. 502, 20, av. A. Einstein, 69621 Villeurbanne Cédex, France

S. Etienne

Laboratoire de Métallurgie Physique et Sciences des Matériaux, Ecole des Mines, URA CNRS 155, Parc de Saurupt, 54042 Nancy Cédex, France

E. Geissler

Laboratoire de Spectrométrie Physique, UJF Domaine Universitaire, 38401 St Martin d'Hères Cédex, France

Received July 29, 1996; Revised Manuscript Received September 18, 1996[⊗]

ABSTRACT: The density fluctuations in poly(methyl methacrylate) are investigated by small-angle X-ray scattering (SAXS) as a function of temperature and microstructural state with time-resolved accuracy, by means of synchrotron radiation. We show for the first time the differences in electronic density fluctuations between quenched and annealed samples in relation to their dynamic behavior. At low temperature, the microstructural state slightly influences the electronic density fluctuations, whereas differences between both samples appear in the glass transition range. SAXS is thus essentially sensitive to fluctuations of dynamic nature. These features are understood and related to the differences observed directly in the relaxational behavior, as revealed by high resolution mechanical spectroscopy and differential scanning calorimetry measurements.

Introduction

The relation between the dynamic behavior and the state of disorder in glassy and liquid systems is the key to understanding glass transition phenomenon. As an example, the free volume theory[1] relates the dynamic properties of the glass transition to the structural parameter v_f (free volume). One can also choose entropy fluctuations,[2] but any description of dynamic-structure relationships with only one order parameter has been shown to be insufficient.[3] Moreover, it is well-known that the molecular motions responsible for the main α-relaxation are cooperative,[4] but how this degree of cooperativity is influenced by the state of disorder is still debated, as experimental evidence of this sensitivity is still lacking.

The structure of disordered condensed matter is characterized by the fluctuation function, $\psi(v)$, as defined by

$$\psi(v) = \frac{\langle N \rangle_v^2 - \langle N^2 \rangle_v}{\langle N \rangle_v} \qquad (1)$$

where N is the number of electrons in the reference volume, v, and $\langle\ \rangle_v$ denotes spatial averaging as the reference volume is moved around the sample. Moreover, we adopt here the idea of Roe and Curro[5] that the density fluctuations can be dynamic (i.e. when a molecular motion occurs, a fluctuation arises from this rearrangement) or static (i.e. that the density fluctuation is not related to a given motion but is "frozen-in"). $\psi(v)$ is thus often written as

$$\psi(v) = \psi_{stat}(v) + \psi_{dyn}(v) \qquad (2)$$

Small-angle X-ray scattering (SAXS) experiments lead to a measurement of $\psi(v=\infty)$ as the extrapolation of the scattered intensity at zero angle, $I(q=0)$, is proportional to $\psi(v=\infty)$.[6,7]

The decomposition of $\psi(v=\infty)$ into its dynamic and static part is in principle possible.[8,9] Below the glass transition temperature T_g, in the glassy frozen-in state, it is observed that $\psi_{stat}(v=\infty)$ is constant. Above T_g, there is a pronounced increase of the dynamic fluctuations, together with the decrease of the static part.

The aim of this contribution is to present accurate scattering results as a function of temperature, by means of synchrotron radiation. The relaxational dynamic behavior is also revealed by low-frequency mechanical spectroscopy. Under the present experimental conditions, the main α and sub-T_g β relaxations, together with the electronic density fluctuations, are investigated and compared for different microstructural states (annealed, quenched) below and above the glass transition. This comparison provides a better understanding of the relations between disorder and degrees of freedom in disordered systems in general.

Experimental Section

Materials under Study. Poly(methyl methacrylate) (PMMA) plates of clinical grade without any additives were

* To whom correspondence should be addressed.

[⊗] Abstract published in *Advance ACS Abstracts,* November 1, 1996.

S0024-9297(96)01145-X CCC: $12.00

purchased from Goodfellow SARL (reference ME303060). The molecular weight was close to 550 000 and the calorimetric T_g of the as-received sample was 388 K, assessed from the onset point determined at 10 K/min heating rate. Isothermal annealing was performed on every sample at $T_a < T_g$. It is well-known that the phenomenon of physical aging will show up as a reduction in volume and enthalpy and that this reduction goes on until metastable equilibrium is reached. Nevertheless, the time scales for equilibrium become very long when the aging temperature is lowered, so that it is not usually possible to achieve the equilibrium state more than 15−20 K below T_g, for accessible times. On the other hand, the variation of enthalpy and volume are rather large as the system is brought far from equilibrium. To induce maximum structural relaxation strength,[10] aged samples were annealed at a temperature of 368 K (T_g − 20 K) for 2 months and then the samples were maintained at room temperature for 1 year. So-called quenched samples were obtained by heating the previously annealed samples above T_g at 413 K and then cooling at 10 K/min, in situ.

The dynamic mechanical, calorimetric, and X-ray measurements were first carried out on these aged samples, by increasing the temperature at the same heating rate of 3 K/min, up to 423 K. Then the samples were quenched in the respective instrument. A second series of measurements was performed at the same heating rate of 3 K/min on the quenched samples.

Differential Scanning Calorimetry. Calorimetric experiments were performed with a Perkin-Elmer DSC-7 apparatus, giving access to the temperature range 10−150 °C under a nitrogen atmosphere. This allows the determination of the variation of the heat capacity C_p versus temperature for variable heating or cooling rate.

Mechanical Spectroscopy. Low-frequency dynamic mechanical spectroscopy measurements were obtained by means of a homemade inverted forced torsional oscillation pendulum described elsewhere.[11] It measures the dynamic modulus $G^* = G' + iG''$ in the temperature/frequency windows [100−500 K]/[1−10^{-4} Hz], in a helium atmosphere. The internal friction $tan\ \phi$ is defined as the ratio G''/G'.

Small-Angle X-ray Scattering. SAXS measurements were carried out on the CRG-D2AM beamline at the European Synchrotron Radiation Facility (ESRF) in Grenoble, France.[12] The power of the incident beam allows us to study the evolution of the scattered intensity as a function of temperature at 3 K/min rate with good counting statistics and a short counting time (30 s). The incident wavelength used is λ = 0.136 nm and the scattering vector range q ($q = 4\pi \sin(\theta)/\lambda$) investigated is 0.2−10 nm^{-1}. Measurements were performed by point collimation with a methane−xenon gas detector allowing 1D-localization. Samples were kept in-situ under vacuum in a cryofurnace within the temperature range from 190 to 500 K.

Data processing involves corrections for absorption,[13] background subtraction, solid angle variation with scattering angle, synchrotron intensity decrease, and changes in transmission factor. The determination of the extrapolated value of the intensity at $q = 0$ was carried out by using the semiempirical law[14]

$$I(q) = I(q{=}0)\exp(bq^2) \qquad (3)$$

and by plotting $\log(I(q))$ versus q^2 over a large q range. Such plots exhibit a linear variation regime up to 6 nm^{-1} and allow $I(q{=}0)$ and b to be determined as a function of temperature and microstructural state.

Experimental Results

The differences in enthalpic state between quenched and annealed PMMA samples are shown in Figure 1. The aged sample exhibits a well-defined peak in heat capacity, C_p, which does not exist for the quenched sample. Integration of the difference in C_p between the two samples yields the enthalpy variation on annealing, according to

$$\Delta H_a = \int_{T=283K}^{T=423K} [C_p(T,\text{annealed state}) - C_p(T,\text{quenched state})]\, dT = 2.5\ \text{J/g} \quad (4)$$

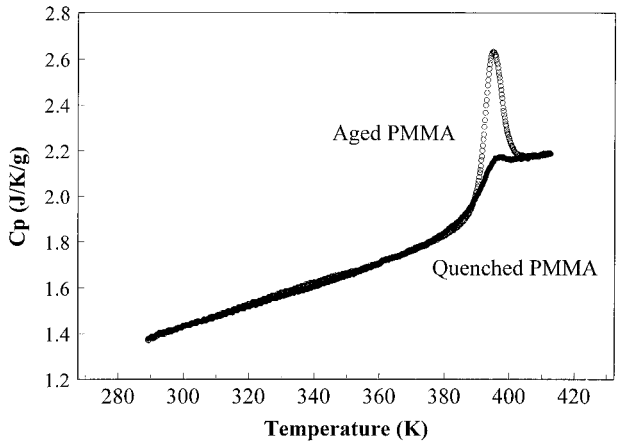

Figure 1. DSC thermograms of aged (○) and quenched (●) PMMA samples obtained with a 3 K/min heating rate.

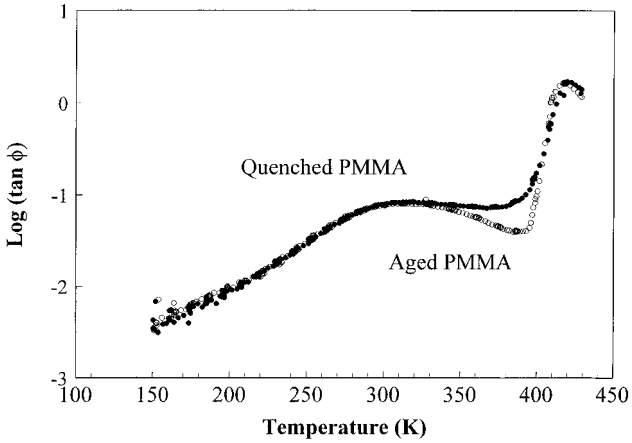

Figure 2. Dynamic mechanical spectrometry measurements at 1 Hz on aged (○) and quenched (●) PMMA, with a 3 K/min heating rate.

Such a structural difference is likely to induce changes in dynamic properties. This is revealed by the shift to higher temperatures of the value of $T_{g(1)}$ on annealing. $T_{g(1)}$ is defined as the onset temperature, *i.e.* the temperature at which the change from the glassy state toward the supercooled liquid becomes detectable.

The change of molecular mobility shows up better with more sensitive methods such as mechanical spectroscopy. The dynamic mechanical behavior of quenched and annealed samples is shown in Figure 2. Both the α and β relaxation are seen on a logarithmic scale. Physical aging has a weak effect on the β process, as localized motions are usually insensitive to microstructure.[15] As a result, the observed differences mainly involve the α relaxation motions below T_g.

The density fluctuations in annealed and quenched PMMA are investigated by SAXS. Figure 3 shows the variation of $I(q{=}0)$ as a function of temperature for both microstuctural states. In agreement with numerous previous studies,[7,16] the results show that density fluctuations increase with increasing temperature below and above the glass transition. Above T_g, the change in the extrapolated intensity with temperature is steeper

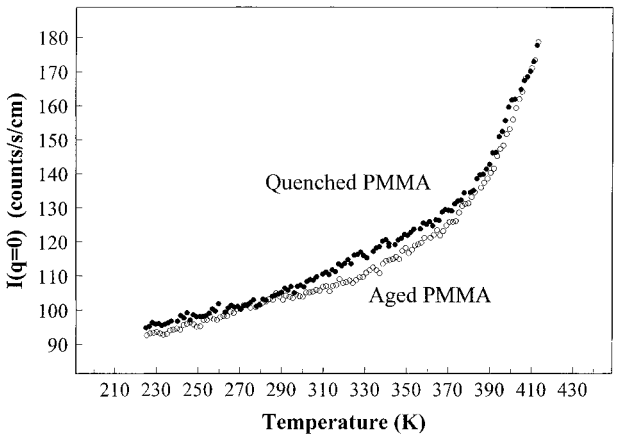

Figure 3. X-ray intensity, $I(q=0)$, obtained by extrapolation of the measured intensity $I(q)$ to zero angle, plotted against temperature, on heating at 3 K/min, for aged (○) and quenched (●) PMMA.

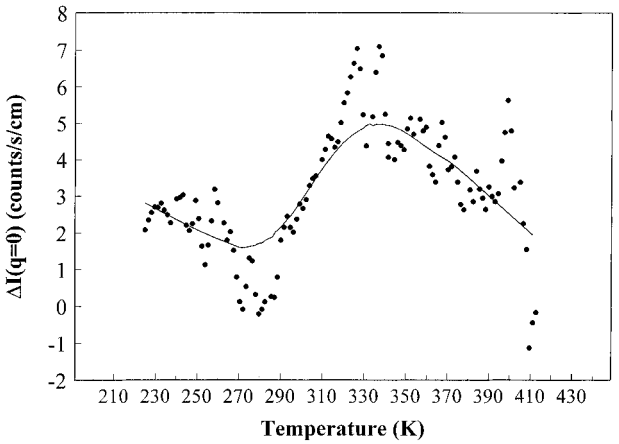

Figure 4. Temperature dependence of $\Delta I(q=0)$ defined as the difference between $I(q=0)$ for quenched and for annealed PMMA. The line represents the smoothing by means of locally weighted regression.

than below T_g. However, the effects of physical aging can be seen only in a limited temperature interval below T_g. In the low-temperature domain (T < 250 K), only a very slight difference in scattering pattern is detected, comparable to the accuracy of measurements. Above room temperature (T > 300 K), the value of $I(q=0)$ is significantly higher for the quenched sample, as the maximum relative difference of extrapolated values is about 7%. Above T_g, both curves merge.

Discussion

Variation of the Static and Dynamic Components of Density Fluctuations. The variation of $I(q=0)$ with temperature was often compared with the temperature dependence of the specific volume.[17−21] Our results indicate that, in contrast to specific volume, no significant changes in density fluctuations between annealed and quenched samples are observable outside the glass transition region, even for long annealing times.[5] Considering that density fluctuations are composed of two distinct contributions (eq 2), we deduce that physical aging mainly influences the dynamic part of density fluctuations observed by SAXS. The temperature range where the increase occurs is a good indication that the associated fluctuations are of a relaxational nature, since a concomitant difference in molecular mobility is observed by low-frequency mechanical spectroscopy, as shown by Figure 2. Changes in the static part, if any, are too small to be observable, compared to the resolution of the measurements. We can see in Figure 1 that below 370 K no enthalpic difference occurs between the aged and annealed sample, implying no structural evolution. Thus, the differences observed in Figure 3 in the temperature range from 300 to 370 K cannot be attributed to any structural change in the static density fluctuations. Consequently, the increase in $\Delta I(q=0)$ defined by

$$\Delta I(q=0) = I(q=0)_{\text{quenched state}} - I(q=0)_{\text{annealed state}} \quad (5)$$

and shown in Figure 4 has to be attributed to a difference in the dynamic component of the fluctuations. Between 370 and 400 K, calorimetric experiments indicate a microstructural evolution of both aged and quenched PMMA samples in order to reach the same equilibrium liquid state at 400 K. In the same temperature range, $\Delta I(q=0)$ decreases progressively and reaches zero at 400 K. Above 400 K, $\Delta I(q=0)$ remains zero as both samples are in the same thermodynamic and structural state. In this high-temperature domain, the dynamic part of the density fluctuations increases as described by statistical thermodynamic theories of liquids,[7] while the static part decreases due to the thawing of the frozen-in density fluctuations.

This interpretation is consistent with recent light-scattering investigations of Yamashita and Kamada[9] showing that, in the temperature domain 300−370 K, the value of the dynamic part of scattered intensity increases with temperature and is higher than the static part. It is thus not surprising that the dynamic density fluctuations play the dominant role in the variation of $I(q=0)$ with temperature and microstructural state. The differences observed here, due to thermal treatments, are also comparable to the kinetic changes of $I(q=0)$ made at the same annealing and measuring temperature by Curro.[17] During physical aging below T_g, a change in microstructure occurs, but as shown above, this would not induce a large change in the static part of the density fluctuations. The decrease in $I(q=0)$ during annealing is more plausibly related to the evolution of the dynamic component of density fluctuations. Thus, no direct relation is to be expected between specific volume relaxation and scattered intensity evolution. Nevertheless, why static density fluctuations remain nearly unchanged by thermal treatments, while significant changes in specific volume can be observed has still to be explained. We can pursue the analysis of dynamic density fluctuations by writing that the dynamic contribution can be separated into three components:

$$\psi_{\text{dyn}} = \psi_\alpha + \psi_\beta + \psi_{\text{vib}} \quad (6)$$

where ψ_α is the part due to α relaxation motions, ψ_β is that due to β relaxation motions, and ψ_{vib} is the part due to vibrational motions. It has already be shown (Figure 2) that the β relaxation[14] and vibrational motions are not significantly affected by physical aging. In contrast, various experiments[22−25] have shown that physical aging significantly affects the α dynamics below T_g. Thus it can be concluded that the evolution of ψ_α is responsible for the observed differences between quenched and annealed samples.

Variation of *b* with Temperature. To determine $I(q=0)$, we use eq 3, which yields the parameter b as a function of temperature. To our knowledge, no previous

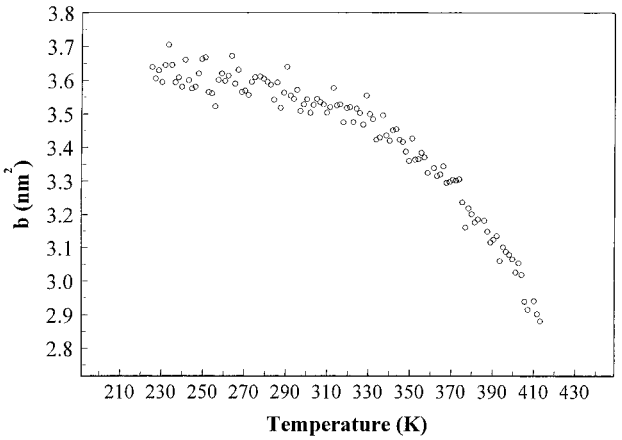

Figure 5. Temperature dependence of the slope, *b*, determined from the plot log($I(q)$) versus q^2, for annealed PMMA sample.

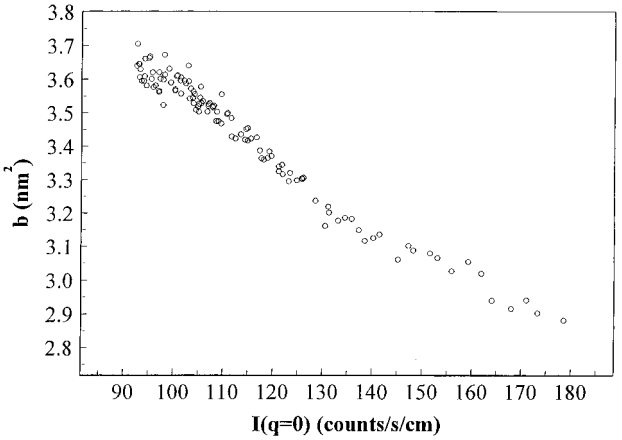

Figure 6. Variation of *b* versus $I(q=0)$ for annealed PMMA sample. These values are determined by fitting the experimental values of $I(q)$ to the equation $I(q) = I(q=0) \exp(bq^2)$ using a least square analysis.

study of the temperature dependence of *b* has been carried out. Nevertheless, it is known[8,14,17] that *b* is the result of positive and negative contributions, namely Compton scattering, thermal diffuse scattering, short range order, a polarization factor, and the atomic structure factor. Figure 5 shows the variation of *b* as a function of temperature for annealed PMMA sample. The value of *b* is roughly constant at low temperatures below 300 K and begins to decrease in the glass transition region. Another way of considering these results is to plot *b* versus $I(q=0)$. As shown by Figure 6, a linear relation between *b* and $I(q=0)$ seems to hold, thus implying that both *b* and $I(q=0)$ have a common physical origin. Accordingly, as $I(q=0)$ depends on the number, the size, and the magnitude of electronic density fluctuations, it can be argued that *b* is also sensitive to the same features. However, the variation of $I(q=0)$ with *b* is essentially due to the change in scattering spectra above T_g, where the fluctuations are dynamic. Thus, the variation of *b* could be related to the specific nature of these fluctuations (dynamic, cooperative).

Conclusion

The present study of electronic density fluctuations observed by SAXS provides evidence of the following.

(i) Annealing essentially influences the dynamic part of the density fluctuations, which implies molecular degrees of freedom related to α-relaxation, whereas no significant change in the static component could be detected. Annealing thus results in very small variations in the quasi-static state of order, but these small changes cause a significant decrease in molecular mobility.

(ii) The values of the parameters $I(q=0)$ and *b* in $I(q) = I(q=0) \exp(bq^2)$ are linearly related, which is still to be associated to a clear physical origin.

The very small modifications observed in $I(q=0)$ after annealing treatment could be explained by the fact that $I(q=0)$ yields information about global density fluctuations in the whole size range (in the thermodynamic limit $v \rightarrow \infty$). It seems to be of interest to examine the details of the short range structure, as the change in disordered matter could be very localized. This requires the study of $I(q)$ over a wider q range (at high scattering angles) in order to obtain $\psi(v)$ for small volumes.[27]

This work will be completed by the study of the effects of plastic deformation on the temperature dependence of scattering pattern. It is known that plastic deformation induces stronger microstructural changes than quenching, and differences in the features of density fluctuations in these two states are also to be investigated.

Acknowledgment. We wish to thank J. P. Simon and J. F. Berar, especially for their help during the experiments. The project was financially supported by the ESRF and this was greatly appreciated.

References and Notes

(1) Cohen, M. H.; Grest, G. S. *Phys. Rev. B* **1979**, *20*, 1077−98.
(2) Adam, G.; Gibbs, J. H. *J. Chem. Phys.* **1965**, *43*, 139−146.
(3) Prigogine, I. *Introduction à la thermodynamique des processus irréversibles*; Dunod: Paris, 1968.
(4) Ngai, K. L.; Wright, G. B. Rep. ACR *(U. S. Off. Nav. Res.* **1984**, 309.
(5) Roe, R.-J.; Curro, J. J. *Macromolecules* **1983**, *16*, 428−34.
(6) Ruland, W. *Prog. Colloid Polym. Sci.* **1975**, *57*, 192−205.
(7) Wendorff, J. H.; Fischer, E. W. *Kolloid-Z. u. Z. Polym.* **1973**, *251*, 876−883.
(8) Wiegand, W.; Ruland, W. *Prog. Colloid Polym. Sci.* **1979**, *66*, 355−66.
(9) Yamashita, T.; Kamada, K. *Jpn. J. Appl. Phys.* **1993**, *32*, 4622−27.
(10) Perez, J.; Cavaille, J. Y., Diaz Calleja, R.; Gomez Ribelles, J. L.; Monleon Pradas, M.; Ribes Creus, A. *Makromol. Chem.* **1991**, *192*, 2141−61.
(11) Etienne, S.; Cavaillé, J. Y.; Perez, J.; Point, R.; Salvia, M. *Rev. Sci. Instrum.* **1982**, *53*, 1231−1266.
(12) Simon, J. P.; Geissler, E.; Hecht, A. M.; Bley, F.; Livet, F.; Roth, M.; Ferrer, J. L.; Fanchon, E.; Cohen-Addad, C.; Thierry, J. C. *Rev. Sci. Instrum.* **1992**, *63* (1), 1051−54.
(13) Taylor, A. The optimum thickness of flat powder compact. In *An Introduction to X-ray Metallography*; Chapman & Hall LTD: London, 1952.
(14) Rathje, J.; Ruland, W. *Colloid Polym. Sci.* **1976**, *254*, 358−370.
(15) Muzeau, E.; Vigier, G.; Vassoille, R. *J. Non Crystal. Solids* **1994**, *172*−174, 575−79.
(16) Tanabe, Y.; Müller, N.; Fisher, E. W. *Polymer J.* **1984**, *16*, 445−52.
(17) Curro, J. J.; Roe, R.-J. *Polymer* **1984**, *25*, 1424−30.
(18) Curro, J. J.; Roe, R.-J. *J. Polym. Sci. Polym. Phys. Ed.* **1983**, *21*, 1785−96.
(19) Floudas, G.; Pakula, T.; Fischer, E. W. *Macromolecules* **1994**, *27*, 917−22.
(20) Roe, R.-J.; Song, H.-H. *Macromolecules* **1985**, *18*, 1603−09.
(21) Jain, S. C.; Simha, R. *Macromolecules* **1982**, *15*, 1522−25.
(22) Etienne, S. *J. Phys. IV (France)* **1992**, *C2*, 41−50.
(23) David, L.; Etienne, S. *Macromolecules* **1993**, *26*, 4489−98.
(24) David, L.; Etienne, S. *Macromolecules* **1992**, *25*, 4302−08.
(25) G'Sell, C.; El Bahri, H.; Perez, J.; Cavaillé, J. Y.; Johari, G. P.; *Mat. Sci. Eng.* **1989**, *A110*, 223−29.
(26) Floudas, G.; Pakula, T.; Stamm, M.; Fischer, E. W. *Macromolecules* **1993**, *26*, 1671−1675.
(27) Song H.-H.; Roe R.-J. *Macromolecules* **1987**, *20*, 2723−32.

MA961145M